Synthesis and Thermal Behavior of Poly(methyl methacrylate)/Maghnia Bentonite Nanocomposite Prepared at Room Temperature via *In Situ* Polymerization Initiated by a New Ni(II)α-Benzoinoxime Complex

Kamel Ouaad,[1,2] Saïd Djadoun,[1] Hafida Ferfera-Harrar,[1] Nicolas Sbirrazzuoli,[3] Luc Vincent[3]

[1]*Laboratoire des Matériaux Polymères, Faculté de Chimie, USTHB, BP 32, El-Alia, Bab-Ezzouar, Algiers 16111, Algeria*
[2]*Département de Chimie, Faculté des Sciences, Université M'Hamed Bouguera, Avenue de L'Indépendance, Boumerdès 35000, Algeria*
[3]*Laboratoire Chimie des Matériaux Organiques et Métalliques, Institut de Chimie de Nice, Faculté des Sciences, Université de Nice Sophia Antipolis, Nice Cedex-2 06108, France*

Received 17 January 2010; accepted 25 May 2010
DOI 10.1002/app.32872
Published online 24 September 2010 in Wiley Online Library (wileyonlinelibrary.com).

ABSTRACT: Poly(methyl methacrylate) (PMMA) and poly(methyl methacrylate)/clay nanocomposite (PMMA/OBT) were successfully prepared in dioxan at room temperature via *in situ* radical polymerization initiated by a new Ni(II)α- Benzoinoxime complex as a single component in presence of 3% by weight of an organically modified bentonite (OBT) (originated from Maghnia, Algeria) and characterized by FTIR, ^{1}H-NMR and viscometry. Mainly intercalated and partially exfoliated PMMA/OBT nanocomposite was elaborated and evidenced by X-Ray diffraction (XRD) and transmission electron microscopy (TEM). The intrinsic viscosity of PMMA/OBT nanocomposite is much higher than the one of pure PMMA prepared under the same conditions. Differential scanning calorimetry (DSC) displayed an increase of 10°C in the glass transition temperature of the elaborated PMMA/OBT nanocomposite relative to the one of pure PMMA. Moreover, the TGA analysis confirms a significant improvement of the thermal stability of PMMA/OBT nanocomposite compared to virgin PMMA: the onset degradation temperature of the nanocomposite, carried out under nitrogen atmosphere, increased by more than 45°C.
 J Appl Polym Sci 119: 3227–3233, 2011

Key words: poly(methyl methacrylate); nanocomposite; *in situ* polymerization; Ni(II)α- benzoinoxime complex; thermal stability

INTRODUCTION

Extensive research has been carried out in the last decades on the elaboration of polymer-clay nanocomposites involving both thermoplastics and thermosets.[1–4] Many of these polymer-clay nanocomposites show significant improvements mainly in their mechanical, barrier and thermal properties compared to micro and macro composites.[5–8]

Poly(methyl methacrylate) (PMMA) is one of the largely investigated thermoplastic-clay nanocomposites. Various methods of preparation of PMMA/Clay nanocomposites that produced intercalated or exfoliated structures of improved properties have been reported.[9–11]

Significant progresses are recently made in the field of transition metal complexes as catalysts for olefin polymerization.[12–14] However, their combination with organically modified clay have attracted less interest in the preparation of polymer/clay nanocomposites via coordination polymerization owing to its challenging sensitivity problem to moisture and tiny impurities. Several approaches were therefore developed to achieve this kind of nanocomposites. Tudor et al.[15] first treated the layered silicate with a large amount of methylaluminoxane (MAO) and then immobilized the metallocene catalyst on the surface of MAO-modified silicates nanowhiskers to subsequently initiate the polymerization of ethylene. Mariott et al.[16] prepared stereochemically controlled PMMA-exfoliated silicate in which metallocene cationic complexes were effectively anchored inside the silicate galleries via a noncation-exchange approach involving protonolysis. He et al.[17] combined a traditional Ziegler–Natta catalyst with modified-montmorillonite to prepare exfoliated

Correspondence to: S. Djadoun (matpolylab@yahoo.fr).

polypropylene nanocomposites. Zhang and coworkers[18] prepared polyethylene nanocomposites using a Nickel α-diimine complex catalyst (bis(4,4′-methylene-bis-(2,6-diisopropylimino) acenaphthene dibromide ($NiLBr_2$) supported covalently on the $AlEt_3$-activated organoclay. Very recently, Woo and coworkers[19] reported the *in situ* preparation of PMMA/clay nanocomposite using intergallery-anchored Nickel(II)acetylacetonate (Ni $(acac)_2$)/MAO coordination catalyst.

A previous paper,[20] described the polymerization of methyl methacrylate (MMA) with a new neutral Ni(II)α-Benzoinoxime complex (NBO) as a single component initiator via radical redox mechanism in the 25–60°C temperature range. This complex is easy to prepare and soluble in common organic solvents. Moreover, it is air and moisture stable and can be handled easily in open air. To the best of our knowledge, this complex has not been so far used to prepare polymer/clay nanocomposites at room temperature.

Based on these advantages and with the aim to improve the poor heat resistance of virgin PMMA without a significant loss of its exceptional optical clarity, PMMA and nanocomposite based on PMMA and an organically modified Maghnia bentonite (originated from Algeria) were prepared via *in situ* intercalative polymerization initiated by this NBO complex in dioxan at room temperature.

The structure, morphology, and thermal behavior of these materials were investigated by FTIR, ^{1}H-NMR, X-Ray diffraction (XRD), TEM, DSC, and TGA.

EXPERIMENTAL

Materials

Methyl methacrylate (MMA) was distilled under reduced pressure. Ni(II)α-Benzoinoxime (NBO) complex was prepared according to literature.[21] The age of the NBO complex used in this study was 37 months old that has a prominent effect on its activity, as evidenced previously in MMA polymerization.[20]

Bentonite from Maghnia (Algeria) was kindly supplied by Bentonite Company of Algeria and analyzed by the central laboratory of the ENOF. This clay contains SiO_2 (55–65%), Al_2O_3 (12–18%), Fe_2O_3 (1–3%), Na_2O (1–3%), CaO (1–5%), K_2O (0.76–1.75%), and MgO (2–3%).

This bentonite was organically modified by Hexadecylammonium chloride (HDA) as previously reported.[22] The organically modified bentonite (OBT) was dried in a vacuum oven for several days at 75°C and kept in a dessicator.

Preparation of PMMA and PMMA/OBT nanocomposite

PMMA and PMMA/OBT systems were prepared by *in situ* polymerization. MMA polymerization was carried out as previously reported[20] in a bottom flask, equipped with reflux condenser and dropping funnel, under nitrogen and magnetic stirring. At room temperature, the MMA and dioxan (volume ratio 1/1) were introduced into a flask and flushed with oxygen–free nitrogen for 30 min. Concurrently, an appropriate amount of Ni(II)α-Benzoinoxime (NBO) complex (1% w/w) was dissolved in dioxan, placed in the dropping funnel under nitrogen flux and finally added into the mixture flask kept at 30°C for 4 h. The reaction was terminated by exposing to air.

Similarly, PMMA/OBT was prepared by *in situ* polymerization method in dioxan. Organically modified Maghnia bentonite (3% by weight) was dispersed in dioxan under magnetic stirring overnight at room temperature. The clay suspension was then added to MMA solution and stirred vigorously for 24 h under inert atmosphere. The NBO solution was finally added to the mixture allowed to react for 4 h at 30°C.

The polymer and nanocomposite obtained by precipitation in a large excess of methanol were purified by dissolution/precipitation and dried in a vacuum oven at 50°C for several days. The yields obtained for virgin PMMA and PMMA/OBT composite were 9.6% and 5.5%, respectively.

It is well known that the solvent effect together with clay–polymer interactions plays an important role in the control of the morphology and properties of the nanocomposites.

Lim and cowokers[23] reported the effect of water on the intercalation and exfoliation behavior of alkyl ammonium substituted polysilsesquioxane surfactant-modified clay in the preparation of PMMA/MMT nanocomposites via free radical polymerization. Thus, highly intercalated nanocomposites were produced in supercritical $scCO_2$ solvent, while partially exfoliated ones were formed in aqueous $scCO_2$ solvent. On other hand, the activity of the complex NBO towards MMA polymerization was very sensitive to the polarity of the solvent used, as evidenced previously.[20] Indeed, the monomer conversion decreased significantly upon increasing solvent polarity. So, all experiments were carried out exclusively in dioxan that led to the highest yield among several other tested solvents.

Characterizations

FTIR spectra of thin films of PMMA and PMMA/OBT cast from THF solutions onto KBr disks were

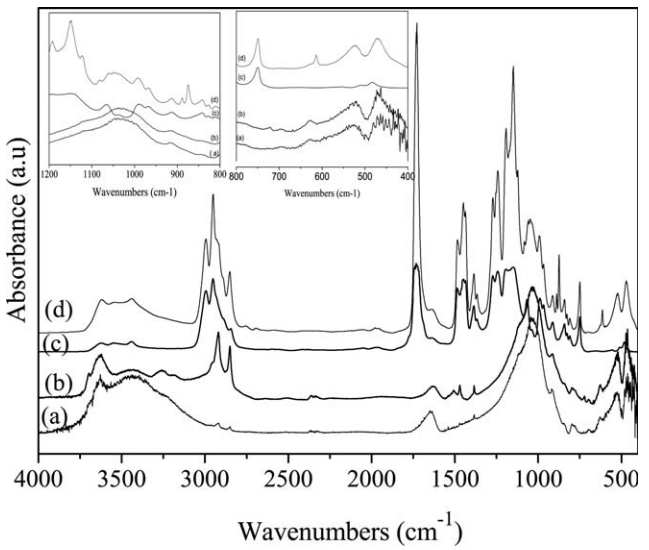

Figure 1 FTIR spectra of (a) pure bentonite (PBT), (b) organo-bentonite clay (OBT), (c) virgin PMMA, and (d) PMMA/OBT composite.

recorded at room temperature on a Perkin–Elmer 1000 one spectrometer. Sixty scans were signal averaged at a spectral resolution of 2 cm^{-1}.

^{1}H-NMR spectra were performed on a Bruker Advanced spectrometer operating at 200 MHz in $CDCl_3$ at 25°C, using tetramethylsilane (TMS) as the internal reference standard.

Viscosity measurements of each polymer were conducted at 30°C in dioxan using an Ubbelhode-Schott Geräte automatic dilution viscometer. Both solution samples were twice prefiltered using swinny stainless Millipore filers (1 and 0.45 μm pore sizes).

X-Ray diffractograms of pure (PBT) and modified Maghnia bentonite (OBT), virgin PMMA and PMMA/OBT composite (prepared in presence of 3% by weight of OBT) were recorded on a Philips PW3710 diffractometer in the range of 2θ (2–50). The monochromatic radiation applied was CuKα ($\lambda = 1.5406$ Å) under 0.5°/min scan rate.

The morphology of the nanocomposites was examined by transmission electron microscopy (TEM) as a complementary technique to XRD on a JEOL 1400 equipped with a MORADA SIS numerical camera at an acceleration voltage of 120 kV.

The glass transition temperatures (T_g) of the synthesized PMMA and its bentonite nanocomposite PMMA/OBT were determined by differential scanning calorimetry using Mettler Toledo 823 DSC under nitrogen at 10°C/min in the range 25–180 °C temperature range. The T_g values were determined at the midpoint of the second scan.

Thermogravimetric experiments were carried out with a Mettler Toledo 851 analyzer using a scanning rate of 10°C/min under air and nitrogen atmosphere in the ranges 30–500°C and 30– 650°C, respectively.

RESULTS AND DISCUSSION

FTIR

Figure 1 shows the FTIR spectra of PBT (pure bentonite), OBT (modified bentonite), virgin PMMA, and PMMA/OBT. The characteristic vibration bands of bentonite are shown at 3630 cm^{-1} (—OH stretching from lattice hydroxyl), 3349 cm^{-1} (—OH stretching from free H_2O), 1036 cm^{-1} (Si—O stretching), 523 cm^{-1} and 470 cm^{-1} (Al—O stretching). The organo-modification of this clay by the ammonium salt (HDA) is in a first step confirmed by FTIR from the appearance of characteristic new bands at 2850 and 2919 cm^{-1} as well as at 1473 cm^{-1} corresponding to the stretching and deformation vibration of the saturated C—H, respectively. The characteristic absorptions of clay (1036, 523 and 470 cm^{-1}) are also observed in the composite sample. This confirms the presence of all components used to prepare the nanocomposite.

^{1}H-NMR analysis

The PMMA obtained with NBO complex in presence of modified bentonite was analyzed by ^{1}H-NMR spectroscopy and compared to pure one. As shown in Figure 2 the ^{1}H-NMR spectrum of PMMA/bentonite system displays singlets at δ 0.98–1.15, 1.95, and 3.72 ppm due to the methyl, methylene and methoxy protons, respectively. In addition to the large absorption of the main chain repeat units, the enlarged spectrum (inset) exhibits the characteristic signal of the intercalation agent (HAD) around 2.38 ppm for the protons of methylene group adjacent to nitrogen of the alkyl ammonium ion, indicating the

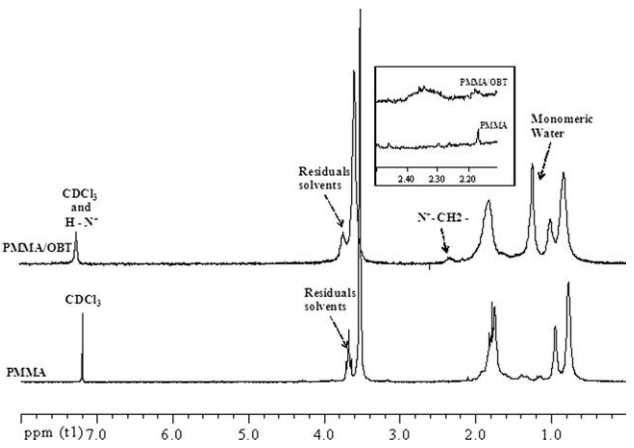

Figure 2 ^{1}H-NMR spectra of PMMA and PMMA/OBT nanocomposite obtained with Ni(II)α-Benzoinoxime complex initiator in $CDCl_3$.

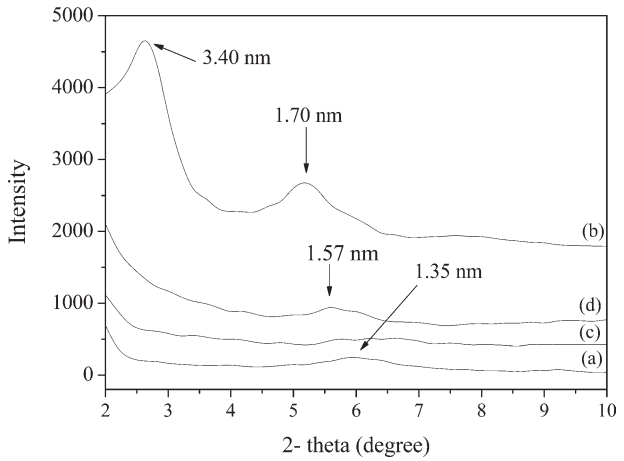

Figure 3 XRD patterns of (a) PBT, (b) OBT, (c) pure PMMA, and (d) PMMA/OBT nanocomposite. (d)-Spacings are indicated in the peak position.

presence of the organophilic clay in polymer matrix. On the other hand, the expected proton signal on the nitrogen of the amine salt in the 6–8.5 ppm range is not observed. However, the striking broadening of solvent peak can be assigned to the interference of these two peaks. It should be noted that the high intensity signal at 1.38 ppm is tentatively ascribed to monomeric water absorption derived from the molecules entrapped in clay galleries during its purification step and the dissolved ones in deuterated chloroform used as solvent. The chemical shifts at 3.8 ppm due to residuals solvents protons (dioxan, methanol) are also observed.

X-ray diffraction

XRD is useful for measurements of d-spacing of intercalated polymer/clay nanocomposites but insufficient for the characterisation of exfoliated ones. The organoclay dispersion has to be checked by both SEM and TEM.

The d-spacing must increase when an intercalated nanocomposite is formed; this latter is evidenced by the appearance of an XRD peak. The absence of XRD peak is however a necessary condition but not sufficient to identify an exfoliated nanocomposite. A mixture of intercalated and exfoliated structures is often observed with nanocomposites.

Figure 3 illustrates the XRD patterns of pristine bentonite, organo-modified bentonite, PMMA and PMMA/OBT composite.

The d_{001} peak of pure Maghnia bentonite appeared as relatively broad at $2\theta = 6.60^\circ$ corresponding to a d-spacing of 1.35 nm. As shown in Figure 3, the increase of the d-spacing observed with OBT (1.70 nm) is an evidence of the intercalation of the HDA ion into the layer of this clay. Virgin PMMA did not show any diffraction peak in the low angle region while a broad weak peak only is observed with PMMA/OBT at an angle of 5.60° relating to a $d_{\text{-spacing}}$ of 1.57 nm, intermediate between those of pure and organo-modified bentonite. This peak may be due to the presence of some unexfoliated tactoids. The absence of the peaks of OBT may be considered at this step as due to the eventual presence of mixed exfoliated and intercalated nanocomposite.

TEM

Complementary information on PMMA/OBT nanomorphology is obtained by TEM. At low magnification (5000 nm scale bar) Figure 4(a), the OBT exists as relatively small tactoids, randomly dispersed and coexisting with some aggregates weakly intercalated within the PMMA matrix. In agreement with XRD, as displayed in Figure 4(b), the formation of intercalated nanocomposite structure is evidenced at higher magnification by the presence of bundles randomly dispersed in the polymer matrix, with thickness ranging from 13 to 32 nm and length varying between 80 and 140 nm and some exfoliated silicate sheets. Moreover, the d-spacing of the silicate layers varied between 2.5 and 5 nm.

In conclusion, mainly intercalated PMMA/OBT nanocomposites coexisting with very small amount

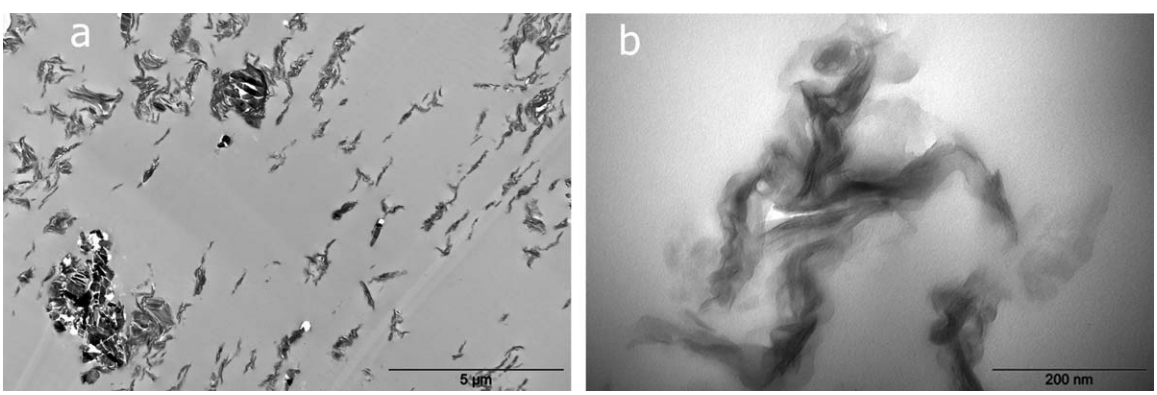

Figure 4 TEM micrographs of PMMA/OBT nanocomposite at (a) 5000 nm scale bar and (b) 200 nm scale bar.

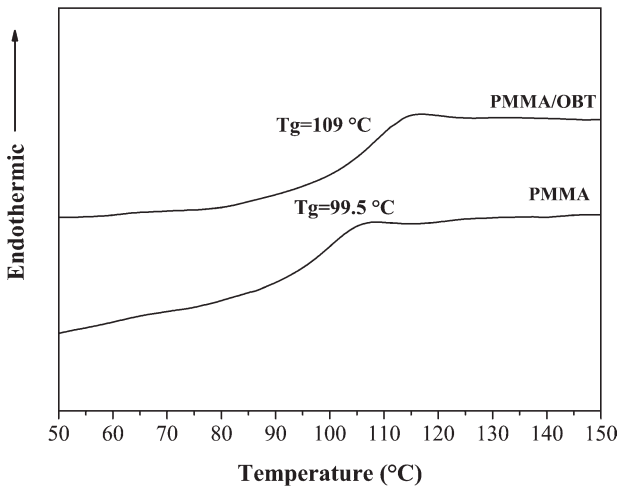

Figure 5 DSC thermograms of pure PMMA and PMMA/OBT nanocomposite.

of exfoliated structures, evidenced from both XRD and TEM techniques were synthesized by *in situ* polymerization at room temperature in dioxan using a new Ni(II)α- Benzoinoxime complex as a single component.

PMMA/MMT intercalated nanocomposites were also synthesized by Huskic and Zigon via one-step *in situ* intercalative polymerization method involving simultaneous modification of MMT with quaternary ammonium salts and polymerization at 70°C using ammonium persulfate as initiator.[24] On the other hand, Tsai et al.[25] prepared PMMA/MMT nanocomposites by *in situ* radical polymerization using cocoamphodipropionate ($C_{24}H_{44}N_2O_6Na_2$) and cocamidopropylhydroxysultaine ($C_{20}H_{42}N_2O_5S$) salts as modifying agents. Conversely, the obtained morphology with same clay loading (3 wt %) was mostly exfoliated due to the presence of acrylic group in the modifiers that provides more compatibility with monomer and sometimes leads to exfoliation.

Viscosimetric measurements

The intrinsic viscosity value of the virgin PMMA of 0.533 dL/g corresponding to a molecular weight, M_v, of 0.234×10^5 g/mol was estimated from Mark-Houwink-Sakurada relationship established by Dondos for PMMA/Dioxan system.[26]

$$[\eta] = 7.7 \times 10^{-2} \; M_v^{0.65} \quad \text{in mL g}^{-1} \qquad (1)$$

In a similar way, intrinsic viscosity measurements were carried out for the PMMA *in situ* polymerized PMMA/OBT nanocomposite. The viscometry solutions filtered twice were homogeneous and clear and led to an intrinsic viscosity of 1.378 dL/g. All large tactoids confirmed by XRD and TEM are expected to be separated; their presence would certainly affect significantly the viscosity measurement and therefore the application of Mark-Houwink-Sakurada equation for molecular weight evaluation. As mainly intercalated PMMA/OBT nanocomposites were elaborated and in agreement with literature reports,[24,27–29] it is difficult to extract the whole fraction of the polymer with intercalated nanocomposite even by heating. The intrinsic viscosity increase of the PMMA synthesized in presence of OBT compared to the virgin one was so important that the presence of any eventual remaining OBT after filtration would not affect significantly the viscosity of the solution. Such increase of intrinsic viscosity may be mainly attributed to an increase of molecular weight. The presence of OBT increased significantly the intrinsic viscosity but reduced the yield by inhibiting the free radical mechanism.[30,31]

DSC analysis

Figure 5 displays DSC thermograms of pure PMMA and PMMA/OBT nanocomposite. The glass transition temperature of the nanocomposite (at the midpoint) of 109°C increased by about 10°C relative to the one of pure PMMA of 99.5°C prepared under the same conditions.

Similar increase of the T_g of PMMA nanocomposites are reported in the literature by several authors[9,24,32,33] as due to the interactions that occurred between the PMMA chains and the OBT layers. The confinement of intercalated polymer chains within the clay galleries which prevents segmental motions of polymer chains may explain the observed increase of the glass transition temperature. Natarajan and coworkers[34] observed however lower T_g of PMMA/clay nanocomposites compared to pure PMMA.

TGA analysis

TGA analysis of PMMA and its corresponding binary nanocomposites was carried out under nitrogen and in presence of air. In general, the degradation under nitrogen atmosphere of PMMA prepared by free radical polymerization occurs in three stages.[35] Indeed as shown in Figure 6, three steps of degradation were observed with virgin PMMA under nitrogen. The first step as a small peak between 100 and 200°C is attributed to the decomposition of the head-to-head linkages in the chain and any eventual traces of impurities or solvent. The second step, as a shoulder that occurred in the 200–300°C region, is initiated by scission at the vinylidene chain-end units. The major decomposition peak, observed around 364°C, is due to random scission of polymer main chain. Such degradation behavior is also

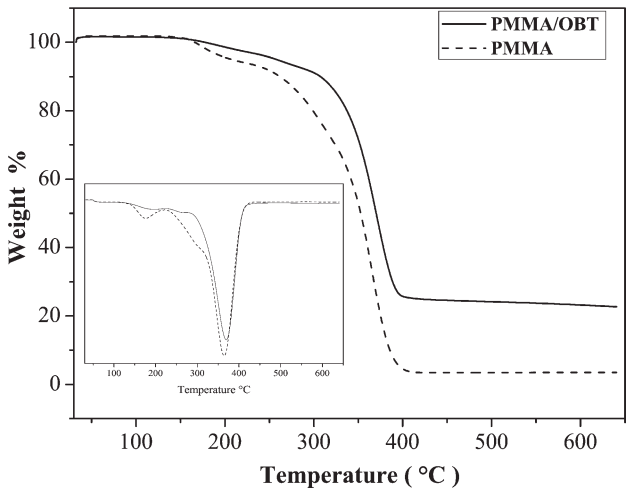

Figure 6 TG and d(TG) curves of virgin PMMA and PMMA/OBT nanocomposite under nitrogen.

considered as an evidence of the mechanism suggested previously.[20]

Figure 6, also confirmed a significant increase of thermal stability of the PMMA/OBT nanocomposite that is mainly attributed to the thermal resistance of OBT and the nanodispersion of OBT sheets in the PMMA matrix. The nanocomposite decomposition appeared to be different from that of virgin polymer. A significant stabilisation occurred in the first and second steps of degradation with the second step mainly due to the decomposition of surfactant which is consistent with literature.[36] Compared to virgin PMMA, the weight loss % of the second step, relative to the vinylidene chain-end degradation, was less significant than that of PMMA. This result provides strong support to the occurrence of irreversible termination polymerization mostly by recombination reactions, which led to higher average molecular weight than disproportion ones, in agreement with

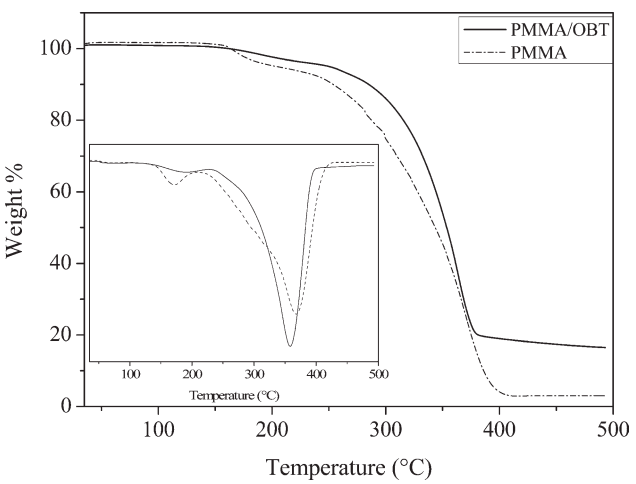

Figure 7 TG and d(TG) curves of virgin PMMA and PMMA/OBT nanocomposite in presence of air.

TABLE I
Thermogravimetric Parameters of PMMA and PMMA/OBT nanocomposite Under Nitrogen Atmosphere and in Presence of Air

Sample/char atmosphere (%)	$T_{d(10\%)}$ (°C)	$T_{d(50\%)}$ (°C)	$T_{d(\max)}$ (°C)
	In presence of air[a]		
PMMA 2.99	253	343	368
PMMA/OBT 16.50	285	354	358
	Under nitrogen[b]		
PMMA 3.48	261	352	364
PMMA/OBT 22.67	307	370	368

[a] Thermogravimetric temperature range 30–500°C.
[b] Thermogravimetric temperature range 30–650°C.

viscosity measurements. The third step which concerns the main chain random scission degradation also shifted to higher temperature. In addition, nano-dispersing OBT sheets prevent the release of degraded PMMA fragments, due to their excellent barrier property, and thus enhanced the overall thermal stability of the system. The fraction that is not volatilized at 650°C $\ll$ char $\gg$ is significant. Similar decomposition behavior with a slight decrease of the thermal stability was observed with PMMA in presence of air, as shown in Figure 7. A broader and higher fraction of PMMA degraded in the second step. The PMMA/OBT nanocomposite showed less thermal stability in the presence of air, while higher char was observed under nitrogen atmosphere.

The overall TGA data shown in Table I where $T_{d(10\%)}$ was considered as a measure of the onset degradation temperature, $T_{d(50\%)}$ as the temperature at which 50% degradation occurred and char at 500°C or 650°C as the amount of material which was not volatile, confirmed the significant enhanced thermal stability of PMMA/OBT compared to virgin PMMA prepared under the same conditions due to the presence of the clay. Intercalated nanocomposites are reported to show better thermal stability than exfoliated ones.[37,38]

CONCLUSION

This study showed that mainly intercalated and partially exfoliated PMMA nanocomposites were successfully prepared by *in situ* polymerization at room temperature in dioxan using a new Ni(II)α-Benzoinoxime complex as a single component in presence of 3% by weight of an organically Maghnia bentonite.

The structure of this nanocomposite was evidenced by FTIR, XRD, and TEM.

The nano-scale dispersion of OBT was evidenced at a macroscopic scale by the significant increase of the T_g of PMMA/OBT nanocomposite, by about 10°C compared to its virgin PMMA and an important improvement of its thermal stability as evidenced by TGA. The onset degradation temperature of PMMA/OBT nanocomposite, carried out under nitrogen atmosphere, was increased by more than 45°C.

Further work on the effects of polymerization media, organo-modified bentonite loading on final PMMA nanocomposites morphologies is in progress. Elaboration of nanocomposites based on other monomers through the same approach is being carried out.

References

1. Pavlidou, S.; Papaspyrides, C. D. Prog Polym Sci 2008, 33, 1119.
2. Ray, S. S.; Okamoto, M. Prog Polym Sci 2003, 28, 1539.
3. Chavarria, F.; Paul, D. R. Polymer 2006, 47, 7760.
4. Kaynak, C.; Nakas, G. I.; Isitman, N. A. Appl Clay Sci 2009, 46, 319.
5. Madbouly, A. S.; Otaigbe, J. U. Prog Polym Sci 2009, 34, 1283.
6. Dzunuzovic, E.; Marinovic-Cincovic, M.; Jeremic, K.; Vukovic, J.; Nedeljkovic, J. Polym Degrad Stab 2008, 93, 77.
7. Chang, C. C.; Hou, S. S. Eur Polym J 2008, 44, 1337.
8. Guigo, N.; Vincent, L.; Mija, A.; Naegele, H.; Sbirrazzuoli, N. Compos Sci Technol 2009, 69, 1979.
9. Oral, A.; Tasdelen, M. A.; Demirel, A. L.; Yagci, Y. Polymer 2009, 50, 3905.
10. Nese, A.; Sen, S.; Tasdelen, M. A.; Nugay, N.; Yagci, Y. Macromol Chem Phys 2006, 207, 820.
11. Jash, P.; Wilkie, C. A. Polym Degrad Stab 2005, 88, 401.
12. Imanishi, Y.; Naga, N. Prog Polym Sci 2001, 26, 1147.
13. Ittel, S. D.; Johnson, L. K.; Brookhart, M. Chem Rev 2000, 100, 1169.
14. Matyjaszewski, K.; Xia, J. Chem Rev 2001, 101, 2921.
15. Tudor, J.; Willington, L.; Hare, D. O.; Royan, B. Chem Commun 1996, 2031.
16. Mariott, W. R.; Chen, E. Y. X. J Am Chem Soc 2003, 125, 15726.
17. He, A.; Hu, H.; Huang, Y.; Dong, J. Y.; Han, C. C. Macromol Rapid Commun 2004, 25, 2008.
18. He, F. A.; Zhang, L. M.; Jiang, H. L.; Chen, L. S.; Wu, Q.; Wang, H. H. Compos Sci Technol 2007, 67, 1727.
19. Cui, L.; Tarte, N. H.; Woo, S. I. J Appl Polym Sci 2008, 110, 784.
20. Harrar-Ferfera, H.; Amrani, F. J Appl Polym Sci 2008, 108, 1514.
21. Hank, Z.; Boutamine, S.; Meklati, M.; Vittori, O. Synth React Inorg Met –Org Chem 1997, 27, 1315.
22. Habi, A.; Djadoun, S.; Grohens, Y. J Appl Polym Sci 2009, 114, 322.
23. Hossain, M. D.; Kim, W. S.; Hwang, H. S.; Lim, K. T. J Colloid Interface Sci 2009, 336, 443.
24. Huskic, M.; Zigon, M. Eur Polym J 2007, 43, 4891.
25. Tsai, T. Y.; Lin, M. J.; Chang, C. W.; Li, C. C. J Phys Chem Solids 2010, 71, 590.
26. Dondos, A. Acta Polym 1994, 27, 1315.
27. Zhang, W.; Li, Y.; Wei, L.; Fang, Y. Mater Lett 2003, 57, 3366.
28. Wang, T. L.; Hwang, W. S.; Yeh, M. H. J Appl Polym Sci 2007, 104, 4135.
29. Wang, H. W.; Shieh, C. F.; Chang, K. C.; Chu, H. C. J Appl Polym Sci 2005, 97, 2175.
30. Meneghetti, P.; Qutubuddin, S. Langmuir 2004, 20, 3424.
31. Solomon, D. H.; Swift, J. D. J Appl Polym Sci 1967, 11, 2567.
32. Hwu, J. M.; Jiang, G. J.; Gao, Z. M.; Xie, W.; Pan, W. P. J Appl Polym Sci 2002, 83, 1702.
33. Xu, Y.; Brittain, J.; Xue, C.; Eby, R. K. Polymer 2004, 45, 3735.
34. Kumar, S.; Jog, J. P.; Natarajan, U. J Appl Polym Sci 2003, 89, 1186.
35. Hirata, T.; Kashiwagi, T.; Brown, J. E. Macromolecules 1985, 18, 410.
36. Gao, Z.; Xie, W.; Hwu, J. M.; Wells, L.; Pan, W. P. J Therm Anal Cal 2001, 64, 467.
37. Gilman, J. W. Appl Clay Sci 1999, 15, 31.
38. Meneghetti, P.; Qutubuddin, S. Thermochim Acta 2006, 442, 74.